# Optimized AVO analysis by using an optimal linear approximation

*M. Riede* & E.Causse, SINTEF Petroleum Research, A.J. van Wijngaarden, Norsk Hydro O&E Research Center, A. Buland, Statoil ASA, J.F. Dutzer, Gaz de France Norge AS, R. Fillon, Gaz de France*

**Summary**

We propose a method, namely OptAVO to build enhanced linear AVO approximations. The basis functions of the approximation are orthogonal and their coefficients represent a new set of AVO attributes. These attributes can directly be used for AVO classification or to obtain better estimates of the usual coefficients (e.g., intercept, gradient). The method will be illustrated for class I reflectors using large reflection angles. A real data example shows the applicability of the proposed approach.

**Introduction**

Amplitudes of reflected and transmitted plane waves at a planar boundary of two elastic media are completely determined for all incidence angles by the Zoeppritz equations (Zoeppritz, 1919), and can be computed if the elastic parameters are known. A number of lineralized approximations to the Zoeppritz equations have been developed that give more insight into the factors that control amplitude changes with offset/angle and simplify computations. Typically, trigonometric functions of the reflection angle are building the basis for the approximations, assuming small elastic parameter changes across the interface (Aki and Richards, 1980) or small incident angles (Ursin and Dahl, 1992). Because of these assumptions the well-known linear AVO approximations can show some inaccuracies, e.g. close to the critical angle. The resulting approximation errors can affect the quality of the AVO analysis, e.g. by causing systematic errors in estimates of the seismic parameter contrasts.
The OptAVO approach still uses a linear approximation, but the trigonometric functions are replaced by more general ones to obtain an optimal approximation. Available information on the seismic parameters is used to derive optimal basis functions for the particular application. The functions are orthogonal and derived using singular value decomposition.

**Method**

A linear AVO approximation using the reflection angle $\theta$, can be written in the general form:

$$R(\theta) \simeq C_1 f_1(\theta) + C_2 f_2(\theta) + C_3 f_3(\theta) + \ldots \quad (1)$$

Setting the basis functions $f_{1,2}(\theta)$ to e.g. $1$ and $\sin^2\theta$ and neglecting the higher order functions we obtain a classical AVO approximation with *intercept* and *gradient* as AVO attributes. To determine the basis functions for the OptAVO approach, we create a set of *N* reference AVO curves by modeling using e.g. the Zoeppritz equations. A realistic distribution, containing the values of the seismic parameters above and below an interface should be available from e.g. information used for rock-physics calibration. Such a distribution is depicted in Figure 1, where shale/sand reflector responses were considered.

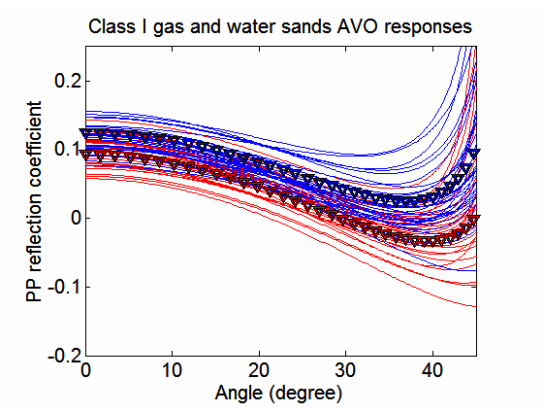


Figure 1: Reference AVO curves for shale/gas-sand (red) and shale/water-sand (blue) reflectors

In each of these models we used the Zoeppritz equations and calculated the curves for a discrete number of angle values. Each reference curve can therefore be represented by a vector. Organizing all vectors as columns in a matrix $\mathbf{R}$ and applying *singular value decomposition* (SVD) we can write:

$$\mathbf{R} = \mathbf{F}\mathbf{D}\mathbf{V}^{\mathrm{T}} = \mathbf{F}\mathbf{W} \quad (2)$$

The matrices $\mathbf{V}$ and $\mathbf{F}$ are orthogonal and $\mathbf{D}$ is diagonal. All matrices are totally defined by the SVD. The new basis functions $f_i(\theta)$ are given by the columns of matrix $\mathbf{F}$ for the discrete reflection angle values used during modeling. Figure 2 shows the basis functions obtained by OptAVO for this particular case. The physical meaning of equation (2) is that, using as many terms as modeled reference curves, each of the reference functions can be exactly described by equation (1), with the coefficients $C_i$, given by the columns of the weighting matrix $\mathbf{W}$. The size of the weights in the matrix is related to the size of the singular values in the diagonal matrix $\mathbf{D}$. As the singular values are sorted in decreasing order the largest weights are associated with the basis functions $f_1$ and $f_2$. As the singular values decrease usually very rapidly, we only need to consider two or three terms in practice. This will introduce only a small

error. The coefficients $C_i$ are representing the new OptAVO attribute space.

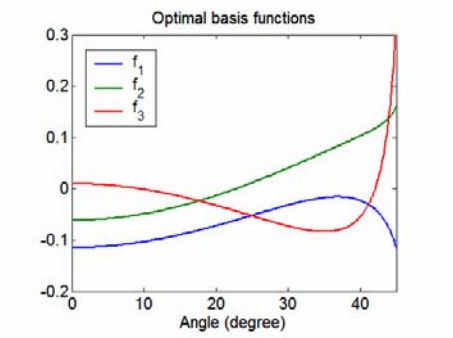


Figure 2: OptAVO basis functions

We should now be able to describe any realistic AVO response that can be expected in the data by inverting for the coefficients $C_i$ using equation (1) and neglecting higher order terms. Figure 3 and Figure 4 show the two-term and the three-term approximations, respectively for a modeled AVO response not contained in the distribution of the reference curves (Figure 1).

The OptAVO approximation is able to represent the increase of amplitude at large reflection angles, since this effect is also present in the reference curves. The usual approximation needs three terms to give a realistic representation at near-critical angles. However, some inaccuracies still remain.

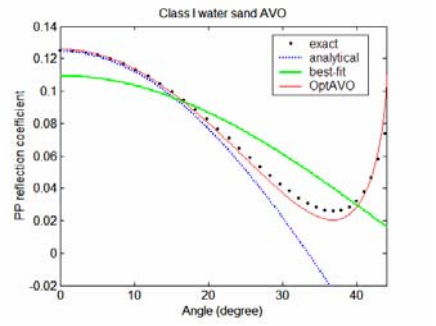


Figure 3: Approximations of a class I shale/water sand AVO curve using two terms. The OptAVO approximation is denoted in red. The doted line shows the exact AVO curve. The blue curve represents the conventional approximation with analytical coefficients taken from the model. The conventional approximation with least-squares coefficients (i.e., chosen to fit the dotted AVO curve) is depicted in green.

The proposed AVO approach using basis functions obtained by SVD can handle various kinds of AVO scenarios and is not restricted to a certain situation. There are in fact no limitations due to large angles, strong contrasts or other effects like anisotropy, as long as an appropriate AVO modeling is done.

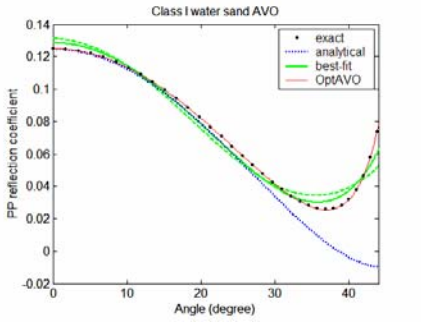


Figure 4: Approximations of a class I shale/water sand AVO curve using three terms.

If we are interested in estimates of the seismic parameter contrast, the OptAVO attributes $C_i$ can be mapped into the conventional AVO attribute space (intercept, gradient, etc.). If the aim is to classify AVO responses the new attributes can be used directly. Further details of the method can be found in Causse and Hokstad (2005), where the same idea is also used for the improved approximation of traveltime-offset curves. Figure 5 shows a crossplot of the OptAVO coefficients $C_1$ vs. $C_2$, indicating the areas where the water sands and gas sands map. This can be used to classify the AVO response of measured data.

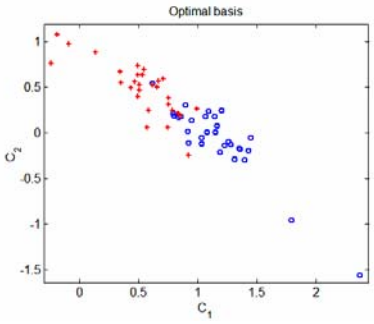


Figure 5: OptAVO attribute ($C_1$,$C_2$) crossplot of reference curves displayed in Figure 1

Different from conventional AVO attributes is that the OptAVO coefficients are not directly related to a physical meaning. However, as already mentioned they can be backprojected to the usual attribute space with intercept ($R_0$) and gradient (G). Figure 6 and Figure 7 show crossplots of intercept vs. gradient obtained by OptAVO. The AVO curves were fitted by the OptAVO approximation with two terms and three terms,

respectively. The estimated coefficients $C_i$ were then converted into estimates of the conventional coefficients by applying a transformation matrix (for details see Causse and Hokstad, 2005).

Note, the good agreement with the analytical calculated values displayed in Figure 8, especially when three terms are used. Figure 9 and Figure 10 which display the results using a usual two/three-term approximation show the inaccuracy of the conventional method. The large angles used in this example results in a large systematic error in the estimated $R_0$ and G values. Using the OptAVO approach we are able to obtain more accurate estimates of $R_0$ and G.

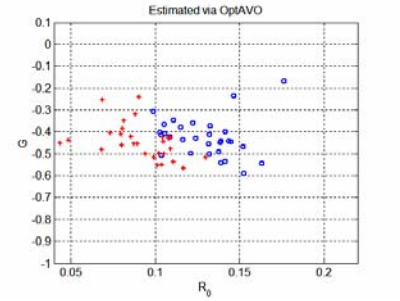


Figure 6: Crossplot of intercept $R_0$ vs. gradient G of the AVO reference curves obtained by OptAVO considering two coefficients ($C_1$, C2)

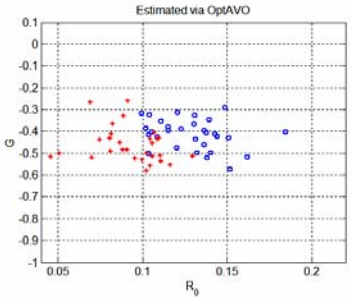


Figure 7: Crossplot of intercept $R_0$ vs. Gradient G of the AVO reference curves obtained by OptAVO considering three coefficients ($C_1$, C2, and C3)

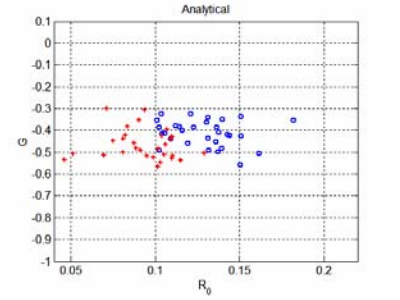


Figure 8: Crossplot of intercept $R_0$ vs. gradient G of the AVO reference curves (**analytical values**).

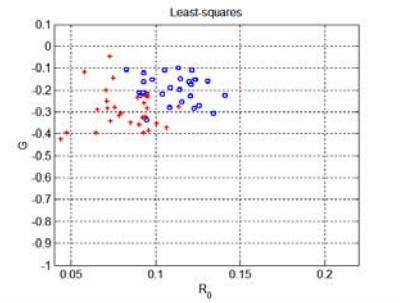


Figure 9: Crossplot of intercept $R_0$ vs. gradient G of the AVO reference curves obtained by usual AVO approximation considering two coefficients.

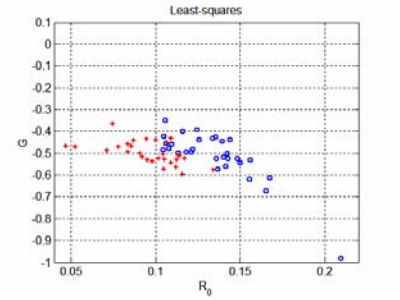


Figure 10: Crossplot of intercept $R_0$ vs. gradient G of the AVO reference curves obtained by usual AVO approximation considering three coefficients.

As the OptAVO basis functions are calculated via SVD they are orthonormal. This means, the values of the estimated attributes are independent of the number of coefficients used in the approximation and the noise is uncorrelated in the crossplots (Cambois, 1998). Thus, stabilizing the AVO analysis with respect to the noise level present in the data becomes easier. Similar advantages can also be obtained by orthogonalizing usual linear approximation basis functions (Herrman and Cambois, 2001) or introducing non-trigonometric orthogonal basis functions (Johansen et al., 1995). However, the OptAVO approach uses an optimal basis of functions to describe AVO responses, with as few coefficients as possible. For a given noise level, we can select the right number of coefficients $C_i$ to use, and drop high-order coefficients associated to components below the noise level.

### AVO classification of field data

To show the practicability of the new method, we used the approach to predict the most likely type of lithology and pore fluids along a seismic section (Figure 11). Compared to the previous example, where only shale/sand class I reflectors were considered, this example uses less constraints. Several reflector types, which are likely to be

present, are considered when constructing the reference AVO models.
The necessary input for the modeling (i.e., mean values and variances of the seismic parameters as a function of depth) were taken from a previous made AVO analysis of the same data set (Avseth et al., 2003).

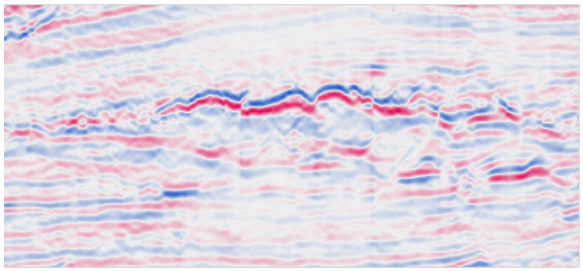

Figure 11: Seismic stack section. (Total time is 0.5 seconds)

The set of modeled AVO reference curves was then used to construct the OptAVO basis functions, which are in that sense optimal for the specific situation. Figure 12 displays a lithology map calculated using the OptAVO attribute sections $C_1$, $C_2$ and performing a classification. We use the *Mahalanobis distance* to estimate the most likely layer category for each data sample. Reflection angles up to 35 degrees were taken into account. Compared to the result constructed with intercept and gradient depicted in Figure 13, OptAVO predicts, in better agreement with well log data, more gas in the top of the reservoir and more oil below (see Avseth et al., 2003). Due to the better lateral continuity of lithologies and pore fluids which can be observed in Figure 12, the OptAVO approach produces a more realistic subsurface map.

## Conclusions

We have presented a method for improved linear AVO approximation. The use of orthogonal basis functions and the optimal adaptation of them to a specific situation by efficient utilization of a-priori information, increase the accuracy of the approximation. Thus, the new AVO attributes extract the information contained in the reflection amplitudes in an optimal and flexible way.
The method can be used to get a better discrimination between different types of AVO responses or to enhance the estimation of conventional attributes like intercept and gradient. The field data example shows the applicability of the method.

## Acknowledgments

We are grateful to Gaz de France, Norsk Hydro and Statoil for financing this work and for the permission to publish these results.

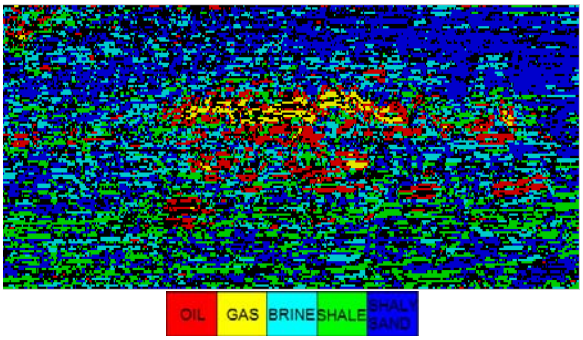


Figure 12: The most likely lithology and pore fluid along the seismic section, obtained by classification of the AVO response using the OptAVO attributes $C_1$ and $C_2$. Black areas correspond to an uncertain classification.

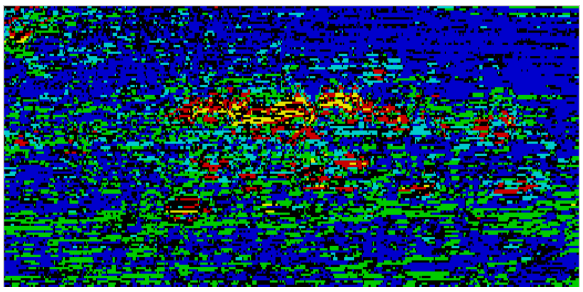

Figure 13: The most likely lithology and pore fluid along the seismic section, obtained by classification of the AVO response using intercept and gradient.

## References

Aki, K.T., and Richards, P.G., 1980, Quantitative Seismology: Theory and Methods: Vol.1, W.H. Freeman and Co.

Avseth, P., Flesche, H. and Wijngaarden, A.J., 2003, AVO classification of lithology and pore fluids constrained by rock physics depth trends, The Leading Edge, 1004-1011.

Cambois, G., 1998, AVO attributes and noise: pitfalls of crossplotting, 68th SEG meeting, 244 -247.

Causse, E., and Hokstad, K., 2005, Seismic processing with general non-hyperbolic travel-time correction, US patent 6.839.658 B2

Herrmann, P. and Cambois, G., 2001, Statistically uncorrelated AVO attributes, 63rd EAGE meeting, P187.

Johansen, T.A., Bruland, L., and Lutro, J., 1995, Tracking the amplitude versus offset (AVO) by using orthogonal polynomials, Geophysical Prospecting, **43**, 245-261.

Ursin, B., and Dahl, T., 1992, Seismic reflection amplitudes, Geophysical Prospecting, **40**, 483-512.

Zoeppritz, K. (1919); Erdbebenwellen VIII b: Über Reflexionen und Durchgang seismischer Wellen durch Unstetigkeitsflächen. Göttinger Nachrichten, **1**:66-84